The Effects of Erythrocyte Membranes on the Nucleation of Sickle Hemoglobin

Alexey Aprelev,* Maria A. Rotter,* Zipora Etzion,† Robert M. Bookchin,† Robin W. Briehl,‡ and Frank A. Ferrone*
*Department of Physics, Drexel University, Philadelphia, Pennsylvania; and †Department of Medicine, ‡Department of Physiology and Biophysics, Albert Einstein College of Medicine, Bronx, New York

ABSTRACT Pathology in sickle cell disease begins with nucleation-dependent polymerization of deoxyhemoglobin S into stiff, rodlike fibers that deform and rigidify red cells. We have measured the effect of erythrocyte membranes on the rate of homogeneous nucleation in sickle hemoglobin, using preparations of open ghosts (OGs) with intact cytoskeletons from sickle (SS) and normal adult (AA) red cells. Nucleation rates were measured by inducing polymerization by laser photolysis of carboxy sickle hemoglobin and observing stochastic variation of replicate experiments of the time for the scattering signals to reach 10% of their respective maxima. By optical imaging of membrane fragments added to a hemoglobin solution we contrast the rate of nucleation immediately adjacent to membrane fragments with nucleation in a region of the same solution but devoid of membranes. From analysis of 29,272 kinetic curves obtained, we conclude that the effect of AA OGs is negligible (10% enhancement of nucleation rates ±20%), whereas SS OGs caused 80% enhancement (±20%). In red cells, where more membrane surface is available to Hb, this implies enhancement of nucleation by a factor of 6. These experiments represent a 10-fold improvement in precision over previous approaches and are the first direct, quantitative measure of the impact of erythrocyte membranes on the homogeneous nucleation process that is responsible for polymer initiation in sickle cell disease.

INTRODUCTION

Sickle cell anemia results from a point mutation on adult hemoglobin molecules, which renders them capable of polymer formation that, in red cells, can lead to vaso-occlusion and shortened red blood cell (RBC) survival. Extensive studies have led to a broad understanding of the polymer formation process in vitro, and it is natural to ask whether there are any significant changes to the process of polymerization in vivo. In particular, it has long been questioned whether the erythrocyte membrane plays a role in the polymerization of sickle hemoglobin. Numerous reports have documented that the membrane interacts differently with hemoglobin S and hemoglobin A (Fung et al., 1983; Liu et al., 1996; Platt and Falcone, 1995; Shaklai et al., 1981), and yet there have been only two published studies directed toward quantifying the effects of the membrane on polymerization, which followed on the initial brief report by Williams and co-worker of an effect of membranes on viscosity of gels (Sundin and Williams, 1976). In one report, Shibata et al. (1980) found that the introduction of membrane fragments from both AA and SS cells diminished the characteristic polymerization time (delay time) of solutions of HbS. Observed delay times decreased by ~25% for each of two added aliquots of membranes. However, the initial concentrations differed for the three kinetic curves presented. Since, under these conditions the delay time varies as roughly the 40th power of the concentration, the difference in the initial concentration alone was sufficient to produce variations of delay times as great as those ascribed to the membrane effects. This placed a somewhat large range of uncertainty on the final results. The second and by far most complete study to date was done by Goldberg et al. (1981). There, an extensive effort revealed an effect on delay times of less than threefold for various preparations of AA membranes, whereas no studies were carried out on membranes from SS cells. In short, the role of the membranes of SS cells in the polymerization process has remained essentially unknown.

It is also very significant that none of these studies was undertaken since the double nucleation mechanism for polymerization was established or its implications understood. It is now known that polymers not only nucleate de novo in solution (homogeneous nucleation), but may also form on the surface of other polymers in a secondary process called heterogeneous nucleation (Ferrone et al., 1985a). Membrane assistance of polymer formation cannot affect this heterogeneous nucleation rate, since by definition it depends on polymers forming on other polymers.

Although membrane-assisted nucleation is conceptually a heterogeneous process, within the formalism describing hemoglobin polymerization it is equivalent to raising the rate of homogeneous nucleation because membrane assistance initiates polymers without the need for other polymers already being present. We will designate homogeneous nucleation or membrane-assisted nucleation as *primary nucleation* in what follows, and reserve the term *heterogeneous nucleation* for nucleation on other polymers.

In typical macroscopic experiments several hundred microliters or more of hemoglobin solution are observed

Submitted August 5, 2004, and accepted for publication December 14, 2004.

Address reprint requests to Frank Ferrone, Dept. of Physics, Drexel University, Philadelphia, PA 19104. Tel.: 215-895-2778; Fax: 215-895-5924; E-mail: fferrone@drexel.edu.

0006-3495/05/04/2815/08 $2.00

doi: 10.1529/biophysj.104.051086

and have many homogeneous nuclei. Nonetheless, the number of heterogeneous nuclei is far greater, and thus most polymers are formed by the heterogeneous nucleation process. Consequently, it is entirely possible to augment new polymer formation (unrelated to other polymers being present) by as much as 10-fold with very little change in the overall kinetics seen in such a macroscopic experiment. On the scale of an erythrocyte, a change in the primary nucleation rates could have profound effects even if macroscopic experiments revealed very little difference. The reason for the difference is that, at the cellular level, it is likely that only one homogeneous nucleus is sufficient to generate all the polymers in a given red blood cell. Consequently, the timing of that singular nucleation event exerts a powerful control over the cell's fate. A nucleus forms by the random coalescence of many monomers, and, as a result, a series of identical experiments on cell-sized volumes exhibits a distribution of formation times. As the nucleation process becomes slower, the distribution of time widens. If nucleation were assisted by a membrane process, this distribution would narrow. What is crucial to the pathophysiology is the net number of events below some critical time, such as the capillary transit (Eaton et al., 1976). Narrowing of the distribution toward the shorter times can therefore cause the number below the critical threshold to rise significantly.

It has long been observed that there is a delay between induction of polymerization and the first detection of polymers (Hofrichter et al., 1974). This delay is now understood to have two components. One is an instrumental effect. From the time when the first nucleus has formed there is a delay before one detects a specific amount of polymer (e.g., 10% of maximum). Because of heterogeneous nucleation, the mass of polymers grows exponentially, making the instrumental delay particularly stark simply due to the nature of exponential growth (Bishop and Ferrone, 1984). Even when a nucleus forms immediately, the exponential growth insures that there is a delay before a signal is observed. In addition, as described above, there may also be a stochastic delay due to randomness in individual nucleation. In macroscopic volumes there are so many nucleation events that enough of them occur in an interval close enough to time zero to polymerize the entire volume in a highly reproducible fashion. Consequently, only the instrumental delay is seen in macroscopic experiments, and the stochastic delay is not observed. But in microscopic volumes, such as those of the red blood cell, the stochastic delay time for the formation of that nucleus can overwhelm the instrumental one. For example, in a 25.5 g/dl sample, the observed macroscopic (instrumental) delay time is ~40 s, whereas in microscopic samples of volumes comparable to erythrocytes the net delay (instrumental plus stochastic) varies from 40 to 200 s. If by some mechanism, such as membrane-mediated nucleation, the primary nucleation rate for this experiment were to increase 10-fold, with all other things remaining equal, the span of delay times on a microscopic sample would collapse—now ranging from 39 to 59 s. The macroscopic delay time would only decrease from 40 s to 39 s, however. This inescapably compromises all macroscopic tests of membrane-assisted nucleation.

Although experiments of high precision might nevertheless discern such subtle differences, attempts to quantify the effect of membranes on nucleation are further confounded by the difficulty of preparing replicate samples for appropriate control experiments. The enormous concentration dependence of the delay time (30–40th power for thermally induced experiments; Hofrichter et al., 1976) means that a 1% error in concentration translates into a 35–49% error in delay time. In the example above, a 10-fold effect on homogeneous nucleation would result in a mere 3% decrease in macroscopic delay, which in turn would easily fall below the limits of precision for most macroscopic experiments, since it would necessitate a replication precision of $>0.1\%$.

This article describes a means by which the previous obstacles can be overcome to provide clear, high-resolution measurements of the effects of membranes on hemoglobin polymerization. It has previously been shown that measurements of stochastic variation of delay times can provide homogeneous nucleation rates despite the presence of abundant heterogeneous nucleation (Cao and Ferrone, 1997; Hofrichter, 1986; Szabo, 1988). To address the issue of precision controls, we directly compare, in the same solution, volumes that contain membranes with volumes that do not. As shown below, the accuracy of the method is better than 1% in homogeneous nucleation rates, which in turn would have required replication accuracy of $<0.02\%$ in concentration if done by conventional means. Using this method, we find significant effects of sickle cell membranes on the rate of nucleation of sickle hemoglobin, and significantly smaller, possibly zero, effects from membranes from cells that contained Hemoglobin A.

MATERIALS AND METHODS

Open ghosts (OGs) were prepared from AA and SS blood, following the procedure of Steck and Kant (1974) as modified by Lew (V. L. Lew, personal communication). Red cells from fresh blood were washed three times in 10 vol of HEPES-buffered (pH 7.5) isotonic saline containing 4 mM KCl and 0.1 mM EGTA, and lightly packed to ~80% Hct by 10 min of centrifugation. After each spin, white cells and platelets were aspirated with the supernatant from the top of the packed cells.

Before lysis, the red blood cells (RBCs) were additionally spun over a cushion of arabinogalactose (Larex, White Bear Lake, MN), with a density of 1.118 g/ml, and the supernatant RBCs remaining above this cushion harvested for the membrane preparations below. This step served to eliminate the dense SS RBC fraction, rich in irreversibly sickled cells (which is also relatively resistant to lysis), and to minimize the marked heterogeneity that might otherwise be obtained with preparations of SS membranes.

The packed cells were lysed in 100 volumes of ice-cold medium L (containing only 2 mM HEPES-Na and 0.1 mM EGTA-Na, pH 7.5–7.7 at 0°C). The lysate was magnetically stirred for ~20 min at 0°C before transferring it to polycarbonate tubes for centrifugation of the ghosts at $30–40 \times 10^3$ *g* for 20 min at 0–4°C. The 0°C incubation in this media free of divalent cations generates a population of inside-out and right-side-out

ghosts (IOGs and ROGs) and allows completion of inside-out eversion in those ghosts which initiated such process after lysis. The supernatant was then aspirated, and the ghosts were washed once more in ice-cold solution L. The transparent polycarbonate tubes permit visualization of the small pale ghost pellet against the dark pink Hb background. Subsequent dilution of the pellet in solution LMg (the same as solution L but with 0.5 mM $MgCl_2$) completely prevents vesiculation and cytoskeletal breakdown, and stabilizes the ghost preparation in the open membrane configuration with conservation of the inside-out or right-side-out topology attained by each ghost during the incubation at 0°C (Lew et al., 1988). Visual confirmation of the grossly open state of IOGs and ROGs prepared with these conditions was obtained by watching 0.4-μm latex particles move freely in and out of these open ghost preparations (V. L. Lew, unpublished observations in video recording). Purified hemoglobin was prepared as previously described (Ferrone et al., 1985b) in 0.05 M phosphate buffer with pH 7.15 and 50 mM sodium dithionite.

Kinetics of polymerization were measured by photolysis of COHbS, using a variation of the stochastic method described elsewhere (Cao and Ferrone, 1997). In brief, a CW-argon laser is split into an array of spots that allow photolysis to be observed separately in ~200 areas. The distribution of delay times gives the homogeneous nucleation rate that is measured here. The specific apparatus utilized an inverted Leica DH-IRB microscope with 20× objectives (Leica, Wetzlar, Germany).

To permit precise comparison of the effect of membranes, two distributions were collected on the same sample region. One distribution was made from photolysis spots that were found not-impinging on membrane fragments; the other distribution was collected from photolysis areas in which a membrane fragment appeared. The membranes could be visualized by observing the sample at the peak absorbance for HbCO, 420 nm, where the hemoglobin is dark and the membranes form lighter regions.

Stochastic variability of the delay has been utilized to measure the rate of homogeneous nucleation. Szabo (1988) has derived an expression for the distribution T of observed delay times t. The homogeneous nucleation rate in a given volume V is denoted by ζ, and B is the rate of exponential growth of the concentration of polymerized monomers. Equation 16 of Szabo (1988) for the distribution of 10th times t (time to reach 1/10 of maximum) can be written as

$$T(t) = \frac{B\Gamma(n+\zeta/B)}{\Gamma(n)\Gamma(\zeta/B)}(1-e^{-\mathrm{Bt}})e^{-\zeta t} = \frac{Bn^{\zeta/\mathrm{B}}}{\Gamma(\zeta/B)}(1-e^{-\mathrm{Bt}})^{\mathrm{n}}e^{-\zeta t}, \quad (1)$$

where Γ is a gamma function. The center expression in this equation is Szabo's original Eq. 16, where the right-hand expression follows when, as is usual, n is large. The parameter n describes the point at which observation is made, and can be shown to be equal to $2\theta\ (c_o–c_s)N_oVB/J$ (F. A. Ferrone, unpublished), in which N_o is Avogadro's number, and J is the net rate of polymer elongation. The values c_o and c_s are initial concentration and solubility of the hemoglobin solution, respectively. The value θ is a threshold parameter, which here is taken as 1/10 for measurements of 10th-time. The value n is large, and lies in the range 10^3–10^6. The distribution described by Eq. 1 begins small because of the $1 - e^{-\mathrm{Bt}}$ term. Once $t > 1/B$, the distribution becomes a decaying exponential, whose decay constant is ζ, the rate of primary nucleation. This gives the distribution its characteristic asymmetric shape. The rate constant for primary nucleation, f_o, measured in mM/s, is related to ζ by

$$\zeta = f_o N_o V, \quad (2)$$

where the constants N_o and V are described above. Since ζ is the parameter obtained by fitting distributions $T(t)$, we can compare rate constants f_o in the presence and absence of membranes only if we correct for the volume that has been occupied by the membrane. It is especially important to compare distributions made from spots with similar volumes because each membrane fragment can occlude a different volume. If the membranes enhance the rate at which the first nucleus forms, then the observed ζ will be increased.

The volume can be determined because the photolyzed area A can be observed directly on the microscope, and the thickness d of the observed region can be inferred by measuring the absorbance of the hemoglobin above and/or below the membrane. Volume V is then equal to $A{\cdot}d$. (With the magnification used here, each camera pixel corresponds to 0.44 μm^2.) Clearly there is no membrane correction for the distributions collected in pure solution. Absorbance measurements were carried out in the Soret band by using a monochromator and a 150-W Xenon lamp for illumination, and a CCD detector. Absorbance differences (with and without photolysis) were computed pixel-by-pixel to determine photolyzed areas.

RESULTS

Fig. 1 shows part of a typical field of view to illustrate the methodology. The photolysis spots are designated as circles and are 5.5 μm in diameter. The membranes (open ghosts) are shown as lighter-colored, and were observed to cluster.

Photolysis experiments were carried out at 34°C on samples between 26.5 g/dl and 28 g/dl. Before collection of kinetics, complete photolysis was verified by absorption measurements in the Soret band. Typical kinetic curves in this experiment are shown in Fig. 2. Only that part of the curve for which the intensity was <10% of its maximum is used in analysis. Each normalized curve was fit to an exponential function $A_s \exp(Bt)$, in which the amplitude A_s differed for each curve but in which B was constrained to be the same for all curves in a given run, whether or not they were in the presence of membranes. The 10th time, $t_{1/10}$, is found by the relation $A_s \exp(Bt_{1/10}) = 0.1$. The constraint on

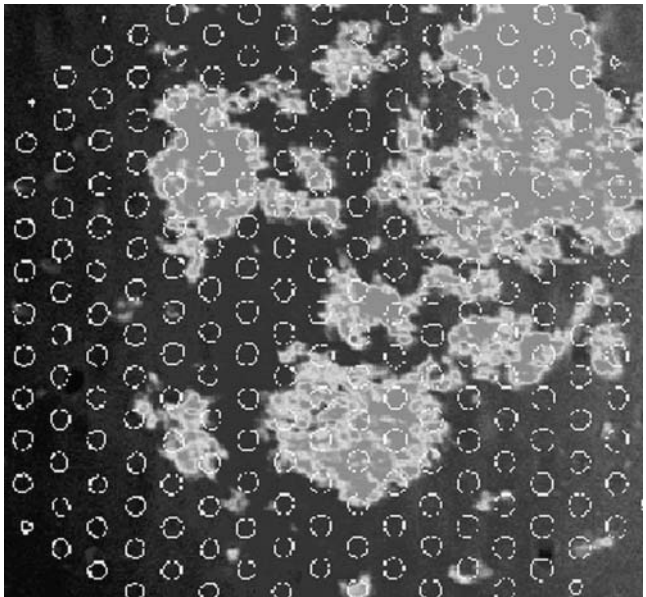

FIGURE 1 Photolysis spots and membrane fragments. The photolysis spots are designated as circles and are 5.5 μm in diameter. The membranes (open ghosts) are shown as lighter-colored, and observed to cluster. The fact that photolysis spots can be identified as devoid of membranes or with membranes present provides a precision control for comparison of their effects.

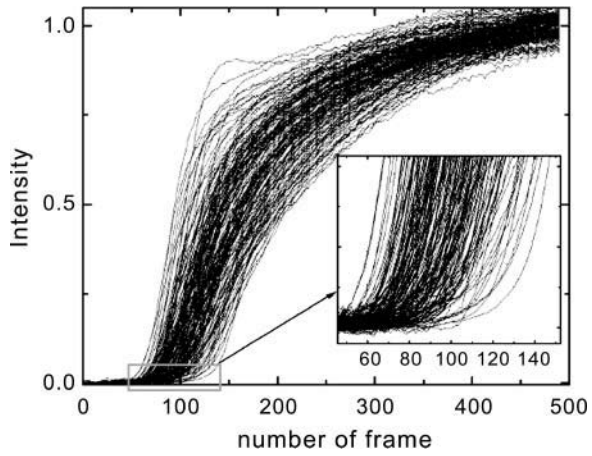

FIGURE 2 Typical kinetic curves. Light scattering intensity at 488 nm is detected in the near forward direction and shown as a function of time after the photolysis begins. The time axis is shown as frames exposed on the camera; the time between frames is 13.2 ms. Only the first 10% of the intensity in a given curve is used in analysis, as shown in the inset. The figure shows 230 curves. Typical rate constants were determined by pooling between 11 and 90 experiments such as the one shown in this figure. Note that the exponential growth is the same in all curves; for fitting, this identity of exponential growth was assumed. Fitting the curves independently gave similar results with slightly lower precision.

the B-values is not essential, but improves the accuracy of the data as determined by refitting the data independently.

To collect a distribution sufficiently large to give precise rates, the experiments were repeated on the same region of the sample, after waiting several minutes between extinguishing the photolysis beam and the start of the next experiment. The exact time was chosen by visually observing in each experiment the disappearance of the photolyzed deoxyHb by its recombination with CO, and then waiting an added time equal to the observed time for religation. Further checks of the delay time distributions confirmed that no residual polymers remained. Stability of the sample over times that range from 100 min to 10.5 h was assured by observing the rate B. Since B is highly sensitive to solution conditions, its constancy assured us of sample integrity. Variation of B was held within 20% of its initial value; a B-value beyond this range was cause for an experimental series to be terminated. (Such a restriction would hold concentration within ~1% of its initial value, for example, if variation in B arose from sample drying.) This permitted collection of >28,000 progress curves in the experiments presented here.

It is evident from Eq. 2 that the volume will affect the distribution. The volume interrogated can depend on the area of the particular beam spot and the amount of membrane in the beam spot in question. We sorted the spots by volume, and constructed paired distributions in which volumes within 5% of each other were employed. In establishing volume, a choice must be made as to how much area of membrane fragments in the beam spot is required to designate a given spot as a member of the distribution of delays potentially affected by the membranes. At one extreme, we can include as membrane-affected those spots where any membrane fragments, no matter how small, lay within the laser-illuminated region. At the other extreme, we may require that the membrane cover the entire spot to be considered one of the membrane-affected class. The results are relatively insensitive to which criterion is used, and we somewhat arbitrarily considered that 30% or more of the area of a spot having membranes would cause that spot to be included in the category of membranes. The ratio of the rate of primary nucleation in the presence of membrane fragments to the same rate without membrane fragments was then computed for all paired volumes (which pairing reduced the overall sample size to ~11,000 kinetic curves). If there is no effect of the membrane constituents, the ratio must be unity; an effect should only enhance nucleation. We are unaware of any way in which the fragments would lessen the rate of primary nucleation (which would provide ratios <1).

Histograms of delay times for two experiments on HbA cells are shown in Fig. 3. The histograms on the left (Fig. 3, *a* and *c*) are those without membranes, whereas the right histogram data (Fig. 3, *b* and *d*) is taken in the presence of membrane fragments. The histograms show an excellent fit to Eq. 1. Each histogram shows the result of a complete experiment in which several exposures were pooled. In each panel, the best fit for the other distribution in the pair (as seen in the adjacent panel) is also shown for comparison and is drawn as a dashed line. Differences between the 10th times for the different experiments represent small concentration errors (of the order of 2%). Note that the intrinsic comparison of areas within the same sample makes such sample-to-sample differences immaterial. Histograms from two experiments on HbS cell membranes are shown in Fig. 4. Again the left panels show the data in the absence of membranes, and the right panels show data with membranes. Note that the high precision of the data permits differences between the distributions to be distinguished clearly.

Systematic differences between SS and AA samples are readily apparent. For those membranes from AA cells, there was almost no membrane effect, and the ratio of nucleation rates is 1.1 ± 0.2. On the other hand, open ghost membrane fragments collected from SS cells enhanced nucleation an average of 80%, having a ratio of nucleation rates of 1.8 ± 0.2.

DISCUSSION

The central finding in the present study is not simply that hemoglobin interacts with the red cell membrane and its components, for indeed there are numerous studies that have reached similar conclusions, as recounted in the Introduction. The contribution of the present work is the quantification of the impact that this interaction has on the polymerization process. This raises four questions: How large is the effect in erythrocytes? How does this compare with previous work?

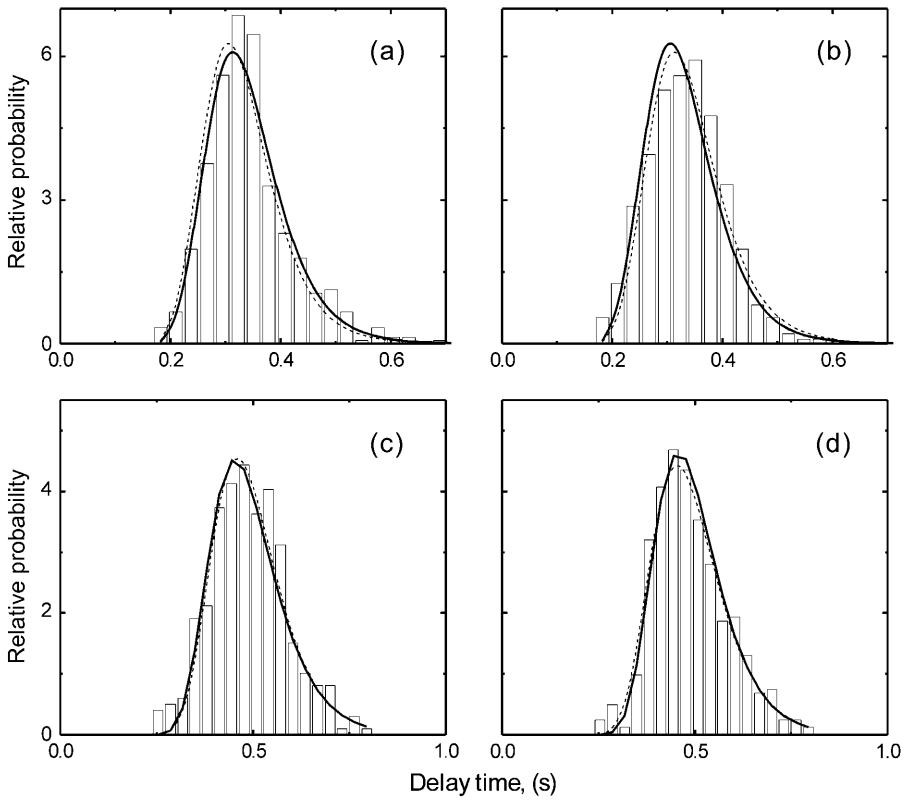

FIGURE 3 Histogram of 10th times for membranes from AA cells. The histograms on *a* and *c* are from data collected where there are no membrane fragments, whereas the histograms on *b* and *d* are collected from photolysis areas that include membrane fragments. The panels *a–d* show 558, 412, 329, and 273 progress curves, respectively. The histograms show excellent fit to Eq. 1. In each curve, the best fit exponential for the *other* distribution in the pair is also shown for comparison, drawn as a dashed line in the particular figure. For the top panel the ratio of homogeneous nucleation rates with membranes to the rates without membranes is 1.1 ± 0.2, whereas the second experiment is 1.2 ± 0.1. Error bars are determined by the quality of the fit. The absence of an effect of membranes on nucleation would give a ratio of 1.

What is the origin of the effect? What are implications for sickle cell disease? We will discuss these in turn.

Size of the effects in vivo

To compare the results at hand to those expected in red cells, we must compare the membrane area available in the two cases since the volumes of Hb are comparable. In the experiments here, the clustering and settling of the membranes means that the typical area available to act as a polymerization initiator is $\sim$24 μm^2, this being the area illuminated by a typical laser spot. Recent measurements of cell surface area are $\sim$142 μm^2 (Gifford et al., 2003). If the nucleation enhancement scales according to area, the effect of membranes on intracellular Hb would be significantly greater than we see here. Thus we would anticipate that in the sickle red cell made of similar SS membranes, primary nucleation would be six times as rapid as in a membrane-free solution.

Previous experiments

As described in the Introduction, there has been one brief report and one abstract describing the effect of SS cell membranes on polymerization, in addition to a thorough study of the effects of AA cells which shares the intrinsic limitation of all experiments using macroscopic volumes attempting to see effects on homogeneous nucleation. Two other, microscopic experiments should be mentioned that might also have been expected to contribute to the question of membrane-assisted nucleation. In the study of Coletta et al. (1982), a series of photolysis experiments on single cells demonstrated that the same kinetic phenomena are seen in cells and in solution—delay times, stochastic variability of the delay, and a high concentration dependence of the delay. These results were critical in establishing that the same general mechanism is operative in cells as in solutions, since these were the phenomena that were essential to developing the double nucleation mechanism. From those experiments, a distribution of intracellular hemoglobin concentrations was deduced which was quite plausible, albeit absent of some high concentration cells reported elsewhere (for a discussion, see Eaton and Hofrichter, 1990). Even though the study employed microscopic volumes, the intracellular concentrations are high enough that most 10th times were not stochastic. As described above, nonstochastic 10th times are not highly sensitive to homogeneous nucleation rates. Moreover, the homogeneous nucleation rates vary by almost 20 orders of magnitude across the range of accessible concentration. In that context, a change of $<$1 order of magnitude will not alter the conclusion that polymerization in cells proceeds by fundamentally the same mechanism as in solutions, nor will it move the distribution by much. The second experiment (Mozzarelli et al., 1987) also involved intracellular photolysis, in which cells at partial saturation were probed for the presence of polymers by observing their delay times. In that experiment, a cell was deemed to have no

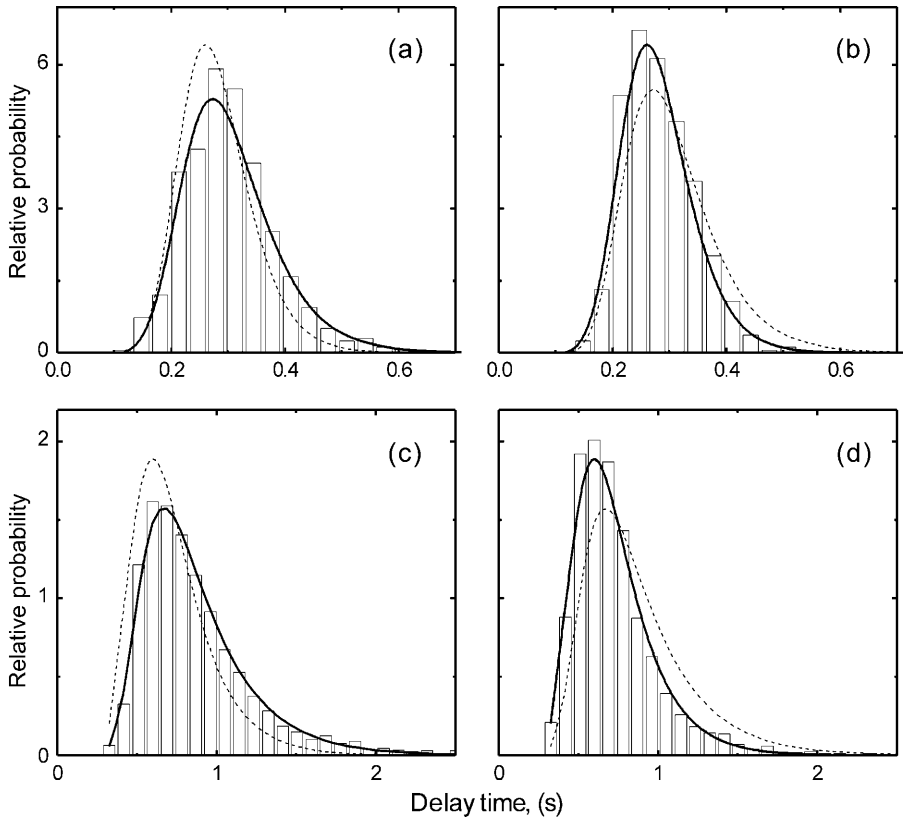

FIGURE 4 Histogram of 10th times for membranes from SS cells. The histograms on *a* and *c* are from data collected where there are no membrane fragments, whereas the histograms on *b* and *d* are collected from photolysis areas which include membrane fragments. Panels *a–d* show 1080, 373, 4394, and 3524 progress curves, respectively. The histograms are fit to Eq. 1. In each curve, the best fit exponential for the *other* distribution in the pair is also shown for comparison, drawn as a dashed line in the particular figure. The effect of the membranes is visually apparent in the difference of the exponential tails of the distribution. For *a* and *b*, the ratio of homogeneous nucleation rates with membranes to the rates without membranes is 2.0 ± 0.2, whereas for *c* and *d*, it is 1.6 ± 0.2. Error bars are determined by the quality of the fit.

polymers when its delay time after polymer melting was the same as it was before melting. There the delay time was again dominated by the instrumental delay, not the stochastic one (otherwise the comparison would be problematic). Hence, although in principle such an experiment might also have had membrane-augmented nucleation, the dominance of heterogeneous nucleation again obscures any membrane effects of the scale seen here. In short, the results here do not stand in opposition to any other data.

Origin of the effect

It is obviously of the greatest interest to determine the features that account for the observed differences between SS and AA membrane effects. In these initial studies, which serve to establish this method, we chose to use open ghosts which retain their cytoskeletons, while allowing full equilibration with concentrated Hb solutions, and to exclude the most dense SS RBCs, to permit greater homogeneity of the SS ghost preparations. There is considerable evidence for structural alterations of SS membranes, including oxidative changes to membrane components, binding of globin (generated when heme is lost, presumably from ferrihemoglobin S), and probably also binding of denatured Hb (Heinz bodies, hemichrome species; Hebbel, 1994). Future experiments with cytoskeletal-free inside-out vesicles, and comparisons between naturally occurring dense SS cells (whose membranes show the greatest extent of the above alterations) and the normodense SS discocytes, as well as experiments with sickle cell trait (AS) membranes, should help narrow down the possible membrane factor(s) contributing to nucleation.

Until the membrane component(s) responsible are identified, it is difficult to establish a mechanism for this process. It is tempting to speculate that it could be similar to the mechanism believed responsible for the process of heterogeneous nucleation of polymers onto previously existing ones. In that case, the cause has been hypothesized to be a contact between a β6 Val on the polymer surface with a hydrophobic pocket (near β88 Leu), which is the same geometry (or nearly so) as that found in the primary contact between HbS molecules within the polymer (Mirchev and Ferrone, 1997). In such a scenario, a small hydrophobic protrusion like the β6 Val or a hydrophobic pocket of comparable size could provide added stability to a cluster formed on the membrane surface, thus increasing the nucleus concentration and hence the rate of nucleation.

Implications

Most fully deoxygenated sickle red cells show delay times <1 s, and thus do not show stochastic delays (Bridges et al., 1996; Coletta et al., 1982). Under such situations, the effects

of augmented homogeneous nucleation on the net delay would be small. However, for deoxygenation at physiologic oxygen pressures, most cells will show delay times >1 s and will therefore be subject to the random variation of delay times. It is for cells with delay times near 1 s that the effects identified here will be greatest. Fig. 5 shows the expected distribution of delay times at 35°C for a concentration of 32.6 g/dl with 50% nonpolymerizing Hb. (This would correspond to ~62% oxygen saturation.) The right curve is that seen in the absence of augmented primary nucleation, and the left curve shows the same parameters except that primary nucleation is sixfold greater. For a capillary transit time of 1 s (shown as the *dashed vertical line*) it is clear that this enhancement has taken a distribution of delay times of which most would not lead to occlusion, and created a distribution where most delay times have occlusive potential. It is therefore of great importance to explore the nature of the effects documented here. Given the profound effects of concentration on the nucleation rate (which varies in some cases as the 50th power of initial concentration; Cao and Ferrone, 1996), it is not immediately apparent how great the physiological significance of the present findings will be. On the one hand, variation in cell concentrations could entirely obscure the effect; on the other hand, if very few cells typically sickle below a critical threshold (such as a 1-s capillary transit), and that average is raised, the effect of membrane-augmented nucleation could be highly significant. Now that an accurate method exists, and effects are known to be present, it is important to determine the scope and nature of the interactions that lead to this increased nucleation rate, to determine how they participate in the disease, and what treatment modalities this new knowledge might suggest.

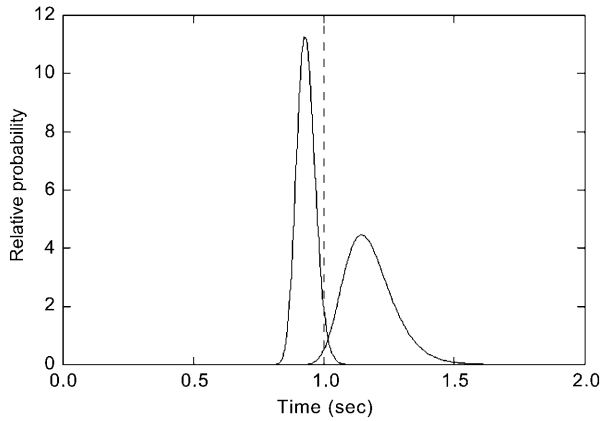

FIGURE 5 Comparison of expected 10th time distributions with and without membrane augmentation. Both curves are drawn using Eq. 1, and only differ in that the left curve has six times the primary nucleation rate of the right curve. Conditions are 35°C, 32.6 g/dl initial concentration, and 50% nonpolymerizing species, corresponding to ~62% oxygen saturation. Each curve shows the relative probability of obtaining a given 10th time shown on the abscissa. The area under both curves is equal, and is unity. The height of the left curve is the consequence of its narrowness. To determine the probability of a delay time in a given interval, the curve must be integrated over the limits dictated by that interval. Hence, even though the *y* axis is >1, the relative probability over any interval will be <1.

We are grateful to Dr. V. L. Lew of the Physiological Laboratory, University of Cambridge, UK, for providing us his tested protocol for preparing the open ghosts employed in this study.

REFERENCES

Bishop, M. F., and F. A. Ferrone. 1984. Kinetics of nucleation controlled polymerization: a perturbation treatment for use with a secondary pathway. *Biophys. J.* 46:631–644.

Bridges, K. R., G. D. Barabino, C. Brugnara, M. R. Cho, G. W. Christoph, G. Dover, B. M. Ewenstein, D. E. Golan, C. Guttmann, and J. Hofrichter. 1996. A multiparameter analysis of sickle erythrocytes in patients undergoing hydroxyurea therapy. *Blood.* 88:4701–4710.

Cao, Z., and F. A. Ferrone. 1996. A 50th order reaction predicted and observed for sickle hemoglobin nucleation. *J. Mol. Biol.* 256:219–222.

Cao, Z., and F. A. Ferrone. 1997. Homogeneous nucleation in sickle hemoglobin. Stochastic measurements with a parallel method. *Biophys. J.* 72:343–372.

Coletta, M., J. Hofrichter, F. A. Ferrone, and W. A. Eaton. 1982. Kinetics of sickle haemoglobin polymerization in single red cells. *Nature.* 300: 194–197.

Eaton, W. A., and J. Hofrichter. 1990. Sickle cell hemoglobin polymerization. *Adv. Protein Chem.* 40:63–279.

Eaton, W. A., J. Hofrichter, and P. D. Ross. 1976. Delay time of gelation: a possible determinant of clinical severity in sickle cell disease. *Blood.* 47:621–627.

Ferrone, F. A., J. Hofrichter, and W. A. Eaton. 1985a. Kinetics of sickle hemoglobin polymerization. II. A double nucleation mechanism. *J. Mol. Biol.* 183:611–631.

Ferrone, F. A., J. Hofrichter, and W. A. Eaton. 1985b. Kinetics of sickle hemoglobin polymerization. I. Studies using temperature-jump and laser photolysis techniques. *J. Mol. Biol.* 183:591–610.

Fung, L. W., S. D. Litvin, and T. M. Reid. 1983. Spin-label detection of sickle hemoglobin-membrane interaction at physiological pH. *Biochemistry.* 22:864–869.

Gifford, S. C., M. G. Frank, J. Derganc, C. Gabel, R. H. Austin, T. Yoshida, and M. W. Bitensky. 2003. Parallel microchannel-based measurements of individual erythrocyte areas and volumes. *Biophys. J.* 84:623–633.

Goldberg, M. A., A. T. Lalos, and H. F. Bunn. 1981. The effect of erythrocyte membrane preparations on the polymerization of sickle hemoglobin. *J. Biol. Chem.* 256:193–197.

Hebbel, R. P. 1994. Membrane-associated iron. *In* Sickle Cell Disease. S. H. Embury, R. P. Hebbel, N. Mohandas, and M. H. Steinberg, editors. Raven Press, New York. 163–172.

Hofrichter, J. 1986. Kinetics of sickle hemoglobin polymerization. III. Nucleation rates determined from stochastic fluctuations in polymerization progress curves. *J. Mol. Biol.* 189:553–571.

Hofrichter, J., P. D. Ross, and W. A. Eaton. 1974. Kinetics and mechanism of deoxyhemoglobin S gelation: a new approach to understanding sickle cell disease. *Proc. Natl. Acad. Sci. USA.* 71:4864–4868.

Hofrichter, J., P. D. Ross, and W. A. Eaton. 1976. Supersaturation in sickle cell hemoglobin solutions. *Proc. Natl. Acad. Sci. USA.* 73:3035–3039.

Lew, V. L., A. Hockaday, C. J. Freeman, and R. M. Bookchin. 1988. The mechanism of spontaneous inside-out vesiculation of red cell membranes. *J. Cell Biol.* 106:1893–1901.

Liu, S. C., S. J. Yi, J. R. Mehta, P. E. Nichols, S. K. Ballas, P. W. Yacono, D. E. Golan, and J. Palek. 1996. Red cell membrane remodeling in sickle cell anemia. Sequestration of membrane lipids and proteins in Heinz bodies. *J. Clin. Invest.* 97:29–36.

Mirchev, R., and F. A. Ferrone. 1997. The structural link between polymerization and sickle cell disease. *J. Mol. Biol.* 265:475–479.

Mozzarelli, A., J. Hofrichter, and W. A. Eaton. 1987. Delay time of hemoglobin S polymerization prevents most cells from sickling. *Science.* 237:500–506.

Platt, O. S., and J. F. Falcone. 1995. Membrane protein interactions in sickle red blood cells: evidence of abnormal protein 3 function. *Blood.* 86:1992–1998.

Shaklai, N., V. S. Sharma, and H. S. Ranney. 1981. Interaction of sickle cell hemoglobin with erythrocyte membranes. *Proc. Nat. Acad. Sci. USA.* 78:65–68.

Shibata, K., G. L. Cottam, and W. R. Waterman. 1980. Acceleration of the rate of deoxyhemoglobin S polymerization by the erythrocyte membrane. *FEBS Lett.* 110:107–110.

Steck, T. L., and J. A. Kent. 1974. Preparation of impermeable ghosts and inside-out vesicles from human erythrocyte membranes. *Methods Enzymol.* 31:172–180.

Sundin, O. H., and R. C. Williams, Jr. 1976. Acceleration of gelation of hemoglobin S by erythrocyte membrane preparations. *Fed. Proc.* 35:1524 (Abstr.).

Szabo, A. 1988. Fluctuations in the polymerization of sickle hemoglobin: a simple analytical model. *J. Mol. Biol.* 199:539–542.